Photoemission Studies of the Alkali Metals. II. Rubidium and Cesium*

Neville V. Smith
Bell Telephone Laboratories, Murray Hill, New Jersey 07974

and

Galen B. Fisher
Stanford Electronics Laboratory, Stanford University, Stanford, California 94305

(Received 7 August 1970)

The photoelectric yield and photoelectron energy distributions have been measured on Rb and Cs in the photon energy range 2.0–11.2 eV. These results and the trends across the series Na, K, Rb, Cs are compared with the predictions of the three-step volume model. The energy distributions show evidence of scattering by pair creation and surface-plasmon creation in close similarity to characteristic energy-loss spectra. Estimates for the hot-electron mean free path in Cs are quite short, indicating that surface properties are likely to be important in some energy ranges.

I. INTRODUCTION

Photoemission experiments have been performed on Rb and Cs using the techniques employed earlier on Na and K.[1] Measurements are reported here for the photoelectric yield and the photoelectron energy distributions taken on thick evaporated films of Rb and Cs in the photon energy range 2.0–11.2 eV. Previous measurements by Ives and Briggs[2] and by Methfessel[3] had been confined to the photon energy range below about 5 eV.

As in the previous paper,[1] the new results will be interpreted in terms of a three-step model[4,5] in which the photoemission process is envisaged as a volume effect occurring in three sequential steps: (a) optical excitation of an electron, (b) transport to the surface, and (c) escape across the surface. If $N_{\rm int}(E, \hbar\omega)$ denotes the internal distribution over energy E of the electrons excited by light of photon energy $\hbar\omega$, the external distribution $N_{\rm ext}(E, \hbar\omega)$ of photoemitted electrons is given by

$$N_{\rm ext}(E, \hbar\omega) = BK(\alpha, l, T_0)\ T_0(E)\ \frac{\alpha l}{1+\alpha l}\ N_{\rm int}(E, \hbar\omega). \tag{1}$$

The simplifying assumptions involved in the derivation of this equation are discussed in the original paper by Berglund and Spicer.[5] The parameters are defined as follows: α is the absorption coefficient of the metal at frequency ω; l is the hot-electron mean free path and is a strong function of E; B is a normalization factor; $T_0(E)$ is a semiclassical threshold function given by

$$T_0(E) = \tfrac{1}{2}\left[1 - \left(\frac{W}{E - E_B}\right)^{1/2}\right] \quad \text{for } E > E_B + W$$
$$= 0 \quad \text{elsewhere.} \tag{2}$$

W is the effective depth of the electron potential well and E_B denotes the energy at the bottom of the free-electron band. The parameter K is a geometrical factor which arises in the spatial and angular integrals and is given by

$$K(\alpha, l, T_0) = \frac{\alpha l + 1}{\alpha l} - \frac{\alpha l + 1}{2T_0(\alpha l)^2} \ln\left(\frac{1+\alpha l}{\alpha l + 1 - 2\alpha l T_0}\right). \tag{3}$$

K is slowly varying the takes on values between $\frac{1}{2}$ and 1. The physical interpretation of Eq. (1) is straightforward. The factor $\alpha l/(1+\alpha l)$ is a measure of the number of photoexcited electrons which reach the surface. Of these, the fraction capable of escaping is given by $T_0(E)$ which is the solid angle of an escape cone divided by 4π.

It is customary to express the above photoemission quantities as numbers of photoelectrons per absorbed photon. The normalization factor B is then given by

$$B^{-1} = \int_{E_F + E_B}^{E_F + \hbar\omega + E_B} N_{\rm int}(E, \hbar\omega)\ dE\ , \tag{4}$$

where E_F is the Fermi energy and takes its free-electron value $\hbar^2 k_F^2/2m$ for the metals under consideration here. The quantum yield expressed in electrons per absorbed photon is then

$$y_{\rm abs} = \int_{E_F + E_B}^{E_F + \hbar\omega + E_B} N_{\rm ext}(E, \hbar\omega)\ dE. \tag{5}$$

This represents the yield of photoelectrons which have emerged from the metal without scattering. Electrons which have undergone a scattering cannot be discarded from the problem. Although the scattering is highly inelastic, the scattered electrons may still be sufficiently energetic to escape from the metal. As in the previous work on Na and K,[1] it will be seen in Sec. IV that the energy distributions contain a very large contribution attributable to secondary electrons which have undergone such

scattering processes. The total yield Y_{abs} is therefore given by y_{abs} plus the yield of secondary electrons.

The Fermi energies in Rb and Cs are quite small, being 1.8 eV in Rb and 1.5 eV in Cs. It will be seen in Sec. IV that the photoelectron energy distributions show a leading peak which falls within the Fermi energy of the high-energy cutoff and can be identified as electrons which have escaped without scattering. The rough separation of the spectra into scattered and unscattered electrons rendered possible in this way enables us to estimate y_{abs}. This in turn leads us to an estimate for the hot-electron mean free path l in Cs at several separate energies. It will be seen that the estimated values of l are extremely short being less than one atomic spacing. The serious implications with regard to the adequacy of the three-step volume model will be discussed.

In Rb and Cs, the low-energy end of the photoelectron energy distributions shows some structure below the leading peak which can be attributed to a discrete energy loss by surface-plasmon creation.[6] In Sec. VI, the photoelectron energy distribution from Cs will be compared with characteristic energy-loss experiments on Na performed by Hölzl, Mayer, and Hoffman.[7]

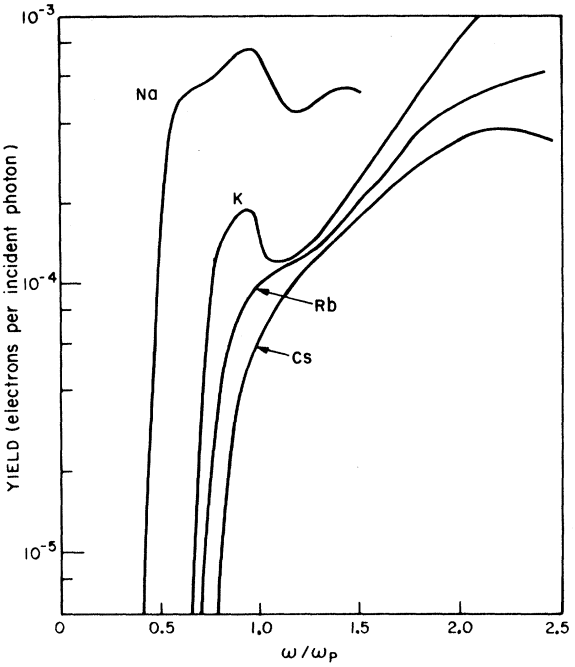

FIG. 2. Photoelectric yield per incident photon for Na, K, Rb, and Cs as a function of the normalized frequency ω/ω_p.

II. EXPERIMENTAL DETAILS

The vacuum chamber and measuring equipment used in these experiments was the same as that used in the work on Na and K.[1] Samples of Rb and Cs were obtained already sealed under vacuum in glass ampules.[8] The quoted purities were 99.95+% for Rb and 99.97% for Cs. An ampule was placed in the vacuum chamber and broken open after the usual pump-down and bakeout procedure. The sample was then prepared by evaporating some of the alkali metal onto a mechanically polished substrate of copper or silver. The results were found to be independent of substrate material. The photoelectron energy distribution curves (EDCs) were measured by the usual ac modulated retarding potential technique.[9] The photoelectric yields were determined by comparing the photocurrent from the sample with the photocurrent from a Cs_3Sb photodiode calibrated by Bauer[10] and by Koyama.[10] The usual correction was made for the transmission of the LiF window.

Rb and Cs are both quite volatile. It was found that after a considerable amount of metal had been released into the chamber, the pressure gradually rose and leveled off near the room-temperature vapor pressure. This presumably represents a situation in which new alkali metal vapor is being evolved as fast as the pump (Varian 110-liter/sec Noble Vacion) can remove it. Layers of alkali metal consequently accumulated on all the internal parts of the chamber giving rise to several troublesome effects. One effect, for example, was to lower the work functions of the internal parts of the chamber and increase their photoelectric yield. Photoelectrons from these surfaces were able to find their way to the emitter and cause a reverse photocurrent. Since the yields of bulk alkali samples are rather small, the reverse current was sometimes comparable with the photocurrent from the sample itself. Reverse photocurrents were accompanied by a distortion of the low-energy end of the measured energy distributions in the form of a

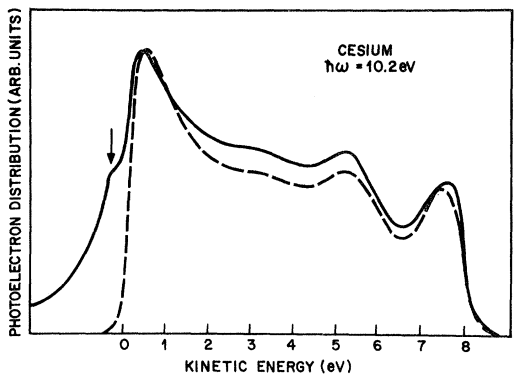

FIG. 1. Photoelectron energy distributions taken on two different samples of Cs. The full curve was taken in the presence of reverse photocurrent and displays a spurious peak indicated by the arrow.

spurious peak. The full curve in Fig. 1 is an EDC taken on Cs while reverse photocurrent was present. The arrow indicates the spurious low-energy peak. The reverse current and spurious peak could be temporarily removed by heating the parts of the chamber in the vicinity of the window in order to disperse the accumulated metal. Only the extreme low-energy end (i.e., below about 0.5 eV in Fig. 1) was affected by this procedure. The broken curve in Fig. 1 shows an EDC taken on a separate sample of Cs in the absence of any measurable reverse photocurrent. The difference between the full and broken curves therefore indicates the reproducibility of the results.

A second troublesome effect was due to condensation of metal on the internal electrical insulators. This gave rise to leakage currents and, in extreme cases, shorted the photocurrent to ground. Heating the appropriate parts in order to disperse the metal was again found to be effective in restoring good performance.

III. PHOTOELECTRIC YIELD

The measured photoelectric yields of Rb and Cs are compared with those of Na and K in Fig. 2. The yields are expressed as Y_{inc}, the number of emitted electrons per *incident* photon, and are plotted against the normalized frequency ω/ω_p where $\hbar\omega_p$ is the plasmon energy taken from measurements by Kunz.[11] In all four metals, the yields are small being generally less than 10^{-3}.

The behavior in the vicinity of the plasmon energy $\hbar\omega_p$ is of particular interest. The values of $\hbar\omega_p$ determined by Kunz from characteristic energy-loss experiments[11] are 5.7, 3.7, 3.4, 2.9 eV, respectively, for Na, K, Rb, and Cs. For Na and K, the yield shows a pronounced drop on passing

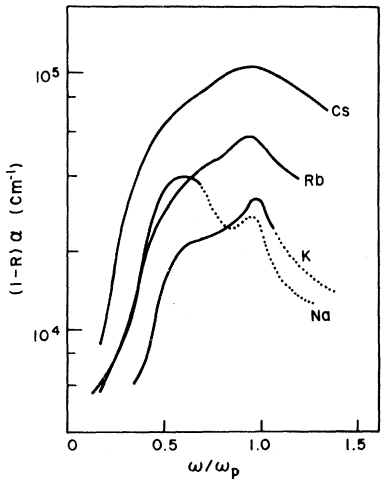

FIG. 3. Variation of $(1-R)\alpha$ for Na, K, Rb, and Cs with the normalized frequency ω/ω_p.

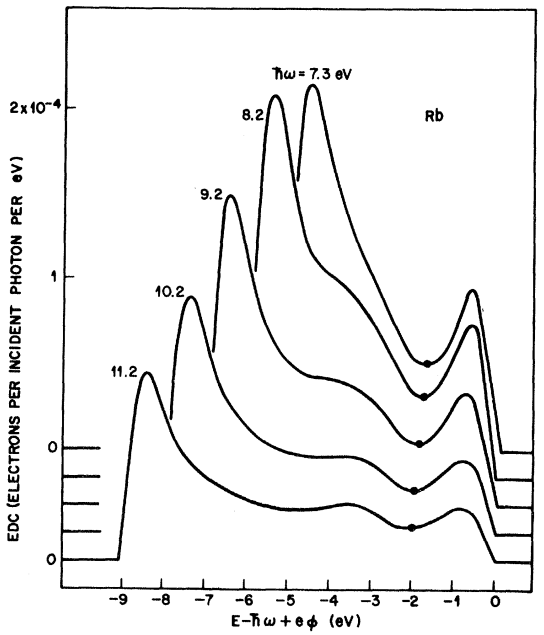

FIG. 4. Photoelectron energy distributions for Rb at high photon energies referred to initial-state energy and normalized to the yield per incident photon.

through the plasma frequency. It was shown in the previous paper that this effect could be understood in terms of the macroscopic optical constants via the function $(1-R)\alpha$, where R is the normal reflectance and α is the absorption coefficient. It is of interest to see if the suggestion of a shoulder in Rb and the absence of structure in Cs near $\hbar\omega_p$ can be understood in the same way.

The $(1-R)\alpha$ factor arises out of the three-step model as follows. First the yield per incident photon, Y_{inc}, is related to the yield per absorbed photon, Y_{abs}, through the absorptance $(1-R)$:

$$Y_{inc} = (1-R)Y_{abs}. \tag{6}$$

Like the unscattered contribution [y_{abs} in Eq. (5)] the scattered contribution to the yield also contains the arrival factor $\alpha l/(1+\alpha l)$. For the electrons under consideration, the mean free path is small and $\alpha l \ll 1$. It follows that the product $(1-R)\alpha$ can be factored out of the expression for Y_{inc}. The optical constants of Rb and Cs have been measured by one of us[12] for frequencies below 4.0 eV. The values of $(1-R)\alpha$ calculated from these optical constants are plotted against ω/ω_p in Fig. 3. The corresponding curves for Na and K are also shown. Each curve shows a peak just below the plasma frequency. The peak arises because $1-R$ increases sharply on passing through the plasma frequency whereas α decreases sharply. The opposing tendencies compensate each other in the product except for the residual peaking effect. The peak,

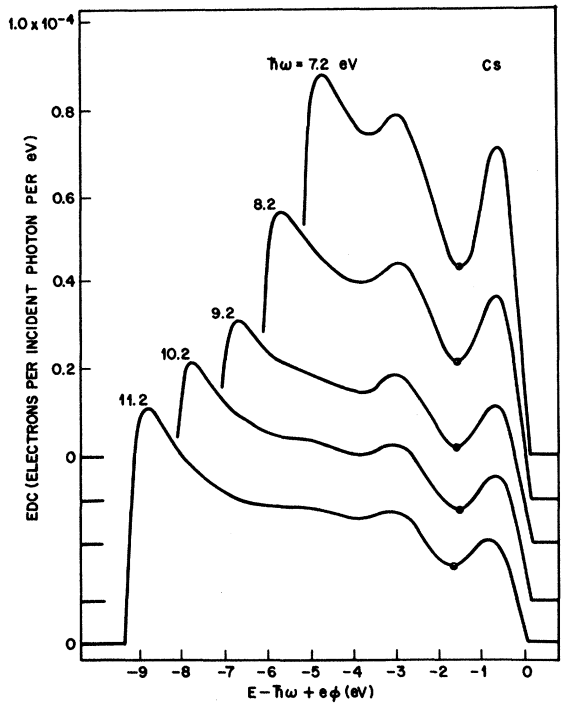

FIG. 5. Photoelectron energy distributions for Cs at high photon energies referred to initial-state energy and normalized to the yield per incident photon.

however, becomes less sharp as we proceed from Na and K to Rb and Cs. This is a consequence of the general broadening of the plasma resonance due to the relatively larger values of ϵ_2, the imaginary part of the dielectric constant.

The increased width of the plasma resonance in Rb and Cs therefore serves to explain the relative lack of structure in Y_{inc} compared with that in Na and K. A second contributing factor is the increasing proximity of the threshold to the plasma frequency. (The values of the work functions deduced from Fowler plots were found to be 2.1 ± 0.1 eV in Rb and 2.0 ± 0.1 eV in Cs.) The rapid falloff of the yield on approaching the threshold will help to obliterate any structure.

IV. PHOTOELECTRON ENERGY DISTRIBUTIONS

In the three-step model, photoelectrons which have escaped from the metal without scattering must lie within the Fermi energy of the high-energy cutoff. The measured photoelectron energy distribution curves (EDCs) taken on Rb and Cs at high photon energies are shown in Figs. 4 and 5, respectively. The curves are plotted against $E - \hbar\omega + e\varphi$, (where E is the electron kinetic energy in vacuum and $e\varphi$ is the work function). This choice of scale refers the photoelectrons to their initial states and places the zero of energy at the Fermi level. The EDCs have been normalized to the yield per incident photon.[13]

It is seen that there is a peak at the high-energy end of the EDCs whose width falls close to the Fermi energy. We therefore identify this peak as electrons which have escaped without scattering. The full circles on the curves represent the estimated position of the minimum in the valley just below the leading peak. In what follows, we will take the valley minimum as the low-energy demarcation of the leading peak. At energies below the leading peak, there are other pieces of structure. The electrons in this region are interpreted as having suffered inelastic scattering before escaping from the metals. Discussion of these electrons, however, will be deferred until a later section. Here, we focus attenuation on the behavior of the leading peak.

The behavior of the leading peak at lower photon energies is illustrated in Figs. 6 and 7. The curves for the lowest photon energies on Cs are similar to those obtained by Methfessel.[3] It is

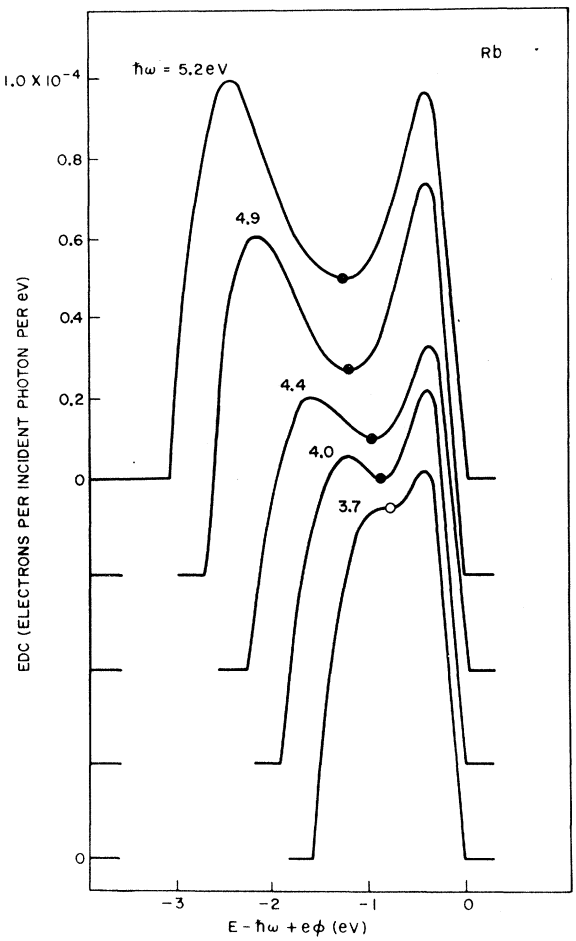

FIG. 6. Photoelectron energy distributions for Rb at low photon energies referred to initial-state energy and normalized to the yield per incident photon.

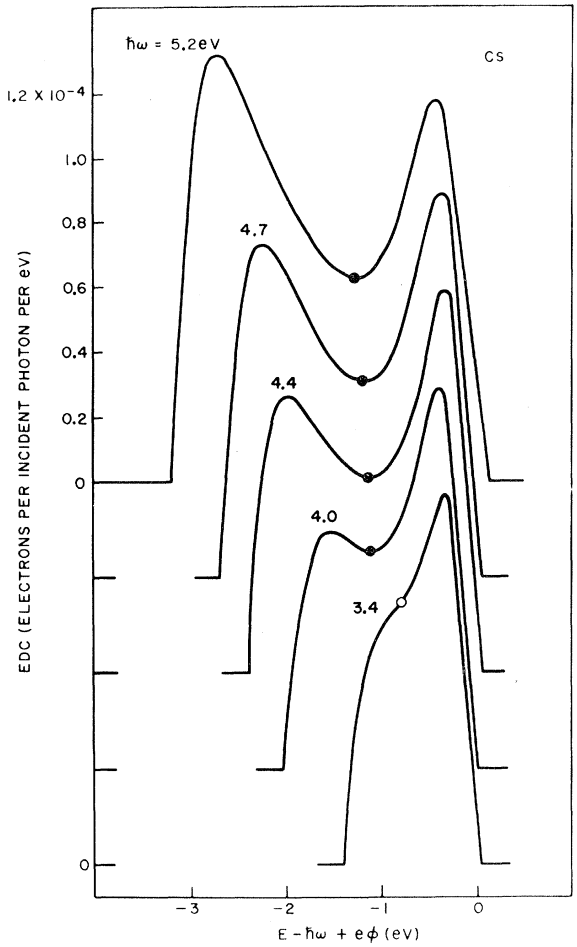

FIG. 7. Photoelectron energy distributions for Cs at low photon energies referred to initial-state energy and normalized to the yield per incident photon.

seen that in both metals, the width of the leading peak decreases with decreasing photon energy. This effect was observed previously[1] in Na and K and it was shown that it could be understood within the framework of the nearly-free-electron model.[14] It was demonstrated that, in order to conserve both energy and momentum, the electrons permitted to participate in optical transitions must lie on a certain plane in k space. The maximum and minimum energies between which the energy of the initial state must fall are given by

$$E_{\max} = E_F = \hbar^2 k_F^2/2m \,, \qquad (7)$$

$$E_{\min} = \frac{2m}{\hbar^2}\left(\frac{\hbar\omega - \hbar^2 G^2/2m}{2G}\right)^2 \,,$$

where $\vec{G}$ is a reciprocal-lattice vector, and k_F is the free-electron Fermi wave number. Curves for $E_{\min}$ are shown in Fig. 8 for both Rb and Cs for the ⟨110⟩ and ⟨200⟩ reciprocal-lattice vectors. The circles in Fig. 8 represent the positions of valleys and points of inflection in the EDCs such as those indicated in Figs. 4–7. It is seen that the narrowing of the leading peak at lower photon energies can be easily understood within the nearly-free-electron model. The shape of the peak, however, is not so successfully explained. The simple model predicts a rectangular shape[1,3] (i.e., the photoelectrons are distributed uniformly in initial energy between the low- and high-energy cutoffs, $E_{\min}$ and $E_{\max}$) whereas the observed peaks are more triangular in shape.

At higher photon energies beyond the minimum in the $E_{\min}$ (110) curve, the experimental points no longer follow the curve. This is not unexpected since the final states involved lie several electron volts above the Fermi level, where the nearly-free-electron model is almost certainly inadequate. Indeed, Ham's band calculations[15] indicate that in the heavier alkali metals, there are flat d-like bands not too far above the Fermi level. It is clear that the simple approach represented by Eq. (1) will be inadequate for transitions involving these bands; and it may be that a calculation using a more realistic representation of these bands would yield better results for the shape of the leading peak. Modification of these upper bands, however, should not affect the narrowing behavior of the peak on decreasing the photon energy.

Other improvements in agreement between theory and experiment may lie in recent theoretical developments by Sutton[16] and by Ashcroft and Schaich.[17] These authors propose models which depart radically from the three-step model and in which the ex-

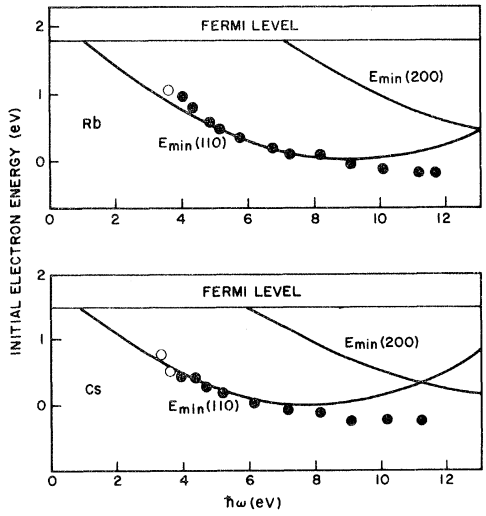

FIG. 8. Frequency variation of $E_{\min}$ for both Rb and Cs taking the zero of energy at the bottom of the band. The smooth curves are calculated; the circles represent the positions of valley minima and points of inflection such as those shown in Figs. 4–7.

istence of the surface plays an important role in the photoemission process. Mahan[18] has shown that proper attention to the angular distribution of photoelectrons can also be important. In particular, Mahan shows that for certain crystal orientations, the surface transmission factors enter into the problem in such a way as to remove the lower edge of the rectangular box shape distribution and give rise to sawtooth-shaped distributions closer to those observed. Experiments on single crystals would be desirable. The samples used in our experiments are believed to be polycrystalline and the preferred directions (if any) are not known. Also, the reflecting properties were not perfectly specular and this would indicate a range of angles of incidence due to nonflatness.

V. ESTIMATES OF HOT-ELECTRON MEAN FREE PATH IN CESIUM

In pursuing an interpretation in terms of the three-step model, we have been led to identify the leading peak in the EDCs as electrons which have escaped without scattering. The area under the leading peak is therefore $y_{\rm inc}$, the yield of unscattered electrons per incident photon, and $y_{\rm inc}$ is equal to $(1-R)y_{\rm abs}$ where $y_{\rm abs}$ is given by Eq. (5). In order to estimate l, let us now introduce the following approximations.

The leading peaks in the EDCs of Figs. 4–7 are seen to be fairly narrow so that we may think of the unscattered electrons as being approximately monoenergetic. At any given photon energy, we may therefore replace the variable functions $T_0(E)$ and $l(E)$ by their values $T_0(\overline{E})$ and $l(\overline{E})$ where $\overline{E}$ is some average energy within the peak. In anticipation, let us assume that the mean free paths are small and that $\alpha l \ll 1$. The factor $\alpha l/(1+\alpha l)$ may be then replaced by αl. It may also be shown that, in this limit, the function $K(\alpha, l, T_0)$ of Eq. (3) may be replaced by $1-T_0(E)$. Combining Eqs. (1), (4), and (5) we have

$$y_{\rm inc} \approx (1-R)(1-T_0)T_0\alpha l . \qquad (8)$$

It follows, therefore, that knowledge of $y_{\rm inc}$, R, T_0, and α leads to estimates for l. The optical constants of Cs measured recently by Whang, Arakawa, and Callcott[19] were used to calculate $(1-R)$ and α. The quantity α is given by $4\pi k/\lambda$, where k is the imaginary part of the refractive index. Values of k were taken from the smooth curve in Fig. 1 of the paper by Whang *et al.* The unscattered yield, $y_{\rm inc}$, was obtained by evaluating the area of the EDCs to the right of the valley minima indicated by full circles in Fig. 7. $T_0(E)$ was evaluated from Eq. (2) with $E=\overline{E}$, taking $\overline{E}$ at about 0.5 eV below the leading edge, and with $W=3.5$ eV. The values of l calculated from Eqs. (8) are plotted against $\overline{E}$ in Fig. 9. Note that the values are extremely short being barely greater than 1 Å.

The shortness of the mean free path casts serious doubt on the validity of the three-step model which assumes that the photoemission process is primarily a volume effect. If the photoelectrons are emerging from only the first atomic layer, it may be more correct to think of photoemission as primarily a surface effect,[16,17,20] at least for Cs at these high photon energies. Rough estimates for Na using the photoemission data of the earlier paper[1] and the optical constants of Sutherland *et al.*[21] also give extremely small mean free paths. If photoemission in the alkali metals is strongly influenced by the surface at these high photon energies, this could explain why the leading peak in the experimental EDCs does not show the rectangular shape predicted by the volume model.

There are, of course, approximations in the model which could lead us to underestimate the mean free path. For example, the semiclassical threshold function of Eq. (2) is based on a crude escape-cone argument which may greatly overestimate the fraction of electrons capable of escaping. Figure 4 of Mahan's paper[18] would indicate that the unscat-

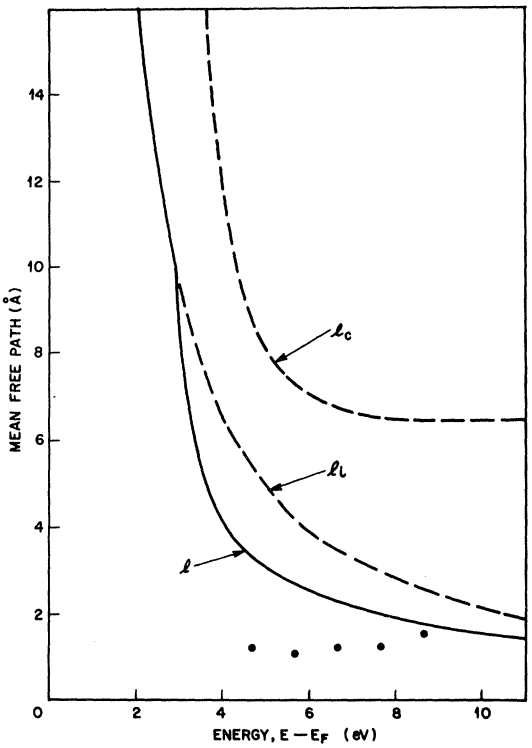

FIG. 9. Experimental and theoretical estimates of the hot-electron mean free path in Cs as a function of energy above the Fermi level. The full circles denote the experimental estimates. The dashed curves represent the contributions due to pair creation (l_i) and plasmon creation (l_c). The full curve (l) represents the combined mean free path.

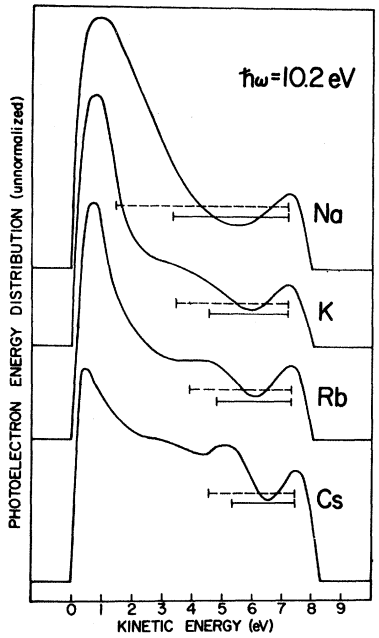

FIG. 10. Photoelectron energy distributions at $\hbar\omega = 10.2$ eV for Na, K, Rb, and Cs. The full horizontal bars represent the surface-plasmon energies; the dashed bars represent the volume-plasmon energies.

tered yield can vary by an order of magnitude depending on crystal orientation.

There is some theoretical reason to suppose that the mean free path in Cs ought to be small. A hot electron scatters against the particles in the Fermi sea and may decay by either collective interactions (plasmon creation) or by individual particle collisions (pair creation). A theoretical expression for the mean free path due to plasmon creation obtained by Quinn[22] and by Thomas[23] is

$$l_c(E) = 2a_B \frac{y}{y_p}\left(\ln\frac{(1+y_p)^{1/2}-1}{y^{1/2}-(y-y_p)^{1/2}}\right)^{-1} \qquad E > E_F + \hbar\omega_p - E_B$$

$$= \infty \qquad \text{elsewhere} . \qquad (9)$$

a_B is the Bohr radius, $y = (E - E_B)/E_F$, $y_p = \hbar\omega_p/E_F$. E_F equals $\hbar^2 k_F^2/2m$ the free-electron Fermi energy, and E_B is the energy location of the bottom of the free-electron band. An approximate expression for the mean free path due to pair creation[22,24] is

$$l_i(E) = \frac{32 a_B}{K\gamma}\frac{y}{(y-1)^2}, \qquad (10)$$

where

$$K = \arctan\gamma + \gamma/(1+\gamma^2) \qquad (11)$$

and $\gamma = (\pi/\alpha r_s)^{1/2}$, where $\alpha = (4/9\pi)^{1/3}$ and $a_B r_s$ is the radius of a sphere which just encloses the volume occupied by one electron. The combined free path l is given by $l_c l_i/(l_c + l_i)$.

The values of l, l_c, and l_i calculated for Cs are plotted in Fig. 9 where they are compared with the experimental estimates. There is order-of-magnitude agreement which is about as good as one can expect in view of the approximations which have gone into both the theoretical and experimental estimates. Even if the agreement were exact, we could derive little comfort from it, since the shortness of the mean free path tends to undermine the model from which the experimental estimates were obtained. Our safest conclusion from both theory and experiment is that the electron-electron interactions in the alkali metals seem to be quite strong and should possibly be taken account of in the optical excitation event itself.[16,25]

VI. SCATTERED ELECTRONS

Although the discussion in the preceding sections indicates that photoemission from the alkali metals may be primarily a surface phenomenon, the three-step volume model may still be of utility in interpreting the qualitative features of the EDCs. Figure 10 shows the EDCs for $\hbar\omega = 10.2$ eV taken on Na, K, Rb, and Cs. The intermediate piece of structure which appears in K and which becomes progressively more pronounced in Rb and Cs, has been attributed by Smith and Spicer[6] to a discrete energy loss through surface-plasmon creation. The horizontal bars in Fig. 10 indicate the volume- and surface-plasmon energies.[11] The separation of the leading and intermediate peaks in Rb and Cs favors the surface-plasmon mechanism. In fact there is

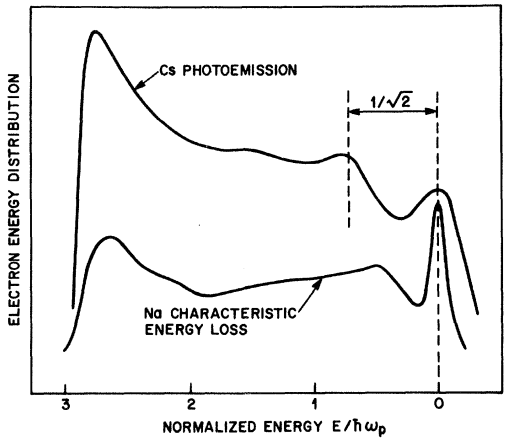

FIG. 11. Comparison between the photoelectron energy distribution of Cs at $\hbar\omega = 11.2$ eV and the characteristic energy-loss spectrum of Na measured by Hölzl *et al.* (Ref. 19) for electrons of 17-eV incident energy. The energy scales have been normalized to the respective plasma frequencies.

nothing in the spectra which can be positively identified as a volume-plasmon loss. The faint piece of structure observable below the intermediate peak in Cs has been tentatively interpreted as either a two-surface-plasmon loss,[6] or the edge of a volume plasmaron.[26]

In the three-step model, we imagine the optical excitation of an electron being followed by a scattering event at some later time. It may be that the optical excitation and scattering events (and also the escape across the surface) are intimately interconnected. For example, in Sutton's many-body surface approach to photoemission,[16] the intermediate peak would be explained as photoelectrons which have left behind a "surface plasmaron" (i.e., a coherently interacting hole and surface plasmon). The experimental results do not distinguish between these alternatives.

The background upon which the surface-plasmon structure is superimposed is attributed to scattering by pair creation. The shape of the background, particularly the low-energy peak, agrees with the predictions of the Berglund-Spicer pair-creation model.[5]

It is of interest to compare the photoemission EDCs with characteristic energy-loss spectra. The comparison will be most meaningful if the characteristic energy-loss experiments were performed with electrons whose incident energy is close to the photon energies used here. Such experiments have been reported on Cs by MacRae, Müller, Lander, Morrison, and Phillips,[27] and they confirm the prominence of surface-plasmon scattering. Measurements have also been reported on Na by Hölzl, Mayer, and Hoffmann.[7] In Fig. 11 we compare these characteristic energy-loss results on Na with the photoemission results on Cs.[28] The horizontal scales have been normalized to the respective volume-plasmon energies taken from Kunz[1] (2.9 eV for Cs, 5.72 eV for Na). The lower curve taken by Hölzl *et al.* is the characteristic energy-loss spectrum of reflected electrons from Na using incident electrons of energy 17 eV. The upper curve is the photoemission EDC taken on Cs at $\hbar\omega = 11.2$ eV and has been placed on the horizontal scale so as to align the leading peaks. The characteristic energy-loss curve on Na shows a peak at energies below the leading peak. This peak is attributed by Hölzl *et al.* to a surface-plasmon energy loss, although its separation is somewhat less than Kunz's value for the surface-plasmon energy, which falls close to the ideal value of $\hbar\omega_p/\sqrt{2}$. As in the photoemission EDCs, the characteristic energy-loss curve shows no peak which can be identified as a volume plasmon. Bearing in mind that the curves in Fig. 11 were obtained in different kinds of experiments on different metals, the similarity is quite striking and suggests that similar basic scattering processes are involved.

VII. CONCLUSION

It has been found that the photoelectric yield and photoelectron energy distributions from Rb and Cs can be understood qualitatively in terms of a three-step volume model which has also worked qualitatively for Na and K. The model, however, runs into difficulties when pushed for quantitative predictions. The lower edge of the predicted rectangular box shape for the distribution of unscattered photoelectrons is not seen in experiment. This discrepancy may be removed by proper attention to the crystal orientation effects in the theory.[18] A more important difficulty with the model, however, is that it leads to estimates of the hot-electron mean free path which are shorter than the atomic spacing. This result, together with the prominence of surface-plasmon structure in the energy distributions, leads us to conclude that photoemission in the alkali metals (at least in Cs at high photon energies) may be more properly thought of as primarily a surface phenomenon. This does not conflict with the earlier work of Piepenbring[29] and Thomas[22] who concluded that photoemission in Na and K is primarily a volume effect. The work of these authors was confined to lower photon energies ($\lesssim 5$ eV) for which the excited electrons have longer mean free paths. We hasten to add also that we have *not* demonstrated here that photoemission in the alkali metals necessarily proceeds via the classic surface photoelectric mechanism treated by Mitchell[20] and others. Our conclusion is merely that both the experimental and theoretical estimates of the mean free path indicate that the majority of photoelectrons, at least for Cs at the higher photon energies, originate from extremely close to the surface and therefore may not be truly representative of the bulb electronic properties.

ACKNOWLEDGMENT

We are grateful to Professor W. E. Spicer for placing the facilities of his laboratory at our disposal, and for valuable discussions.

---

†Work performed while one of the authors (N. V. S.) was on assignment at Stanford University from Bell Telephone Laboratories. The facilities used at Stanford are supported in part by the Advanced Research Projects Agency through the Center for Materials Research at Stanford University, and by the National Science Foundation.

[1] N. V. Smith and W. E. Spicer, Phys. Rev. 188, 593 (1969).

[2] H. E. Ives and H. B. Briggs, J. Opt. Soc. Am. 28,

330 (1938).
[3]S. Methfessel, Z. Physik 147, 442 (1957).
[4]W. E. Spicer, Phys. Rev. 112, 114 (1958).
[5]C. N. Berglund and W. E. Spicer, Phys. Rev. 136, A1030 (1964); 136, A1044 (1964).
[6]N. V. Smith and W. E. Spicer, Phys. Rev. Letters 23, 769 (1969).
[7]J. Hölzl, H. Mayer, and K. W. Hoffmann, Surface Sci. 17, 232 (1969).
[8]Supplied by Atomergic Chemetals Co., Carle Place, L. I., N. Y.
[9]W. E. Spicer and C. N. Berglund, Rev. Sci. Instr. 35, 1665 (1964); R. C. Eden, *ibid.* 41, 252 (1970).
[10]R. S. Bauer (private communication); R. Y. Koyama, thesis (Stanford University, 1969) (unpublished).
[11]C. Kunz, Z. Physik 196, 311 (1966).
[12]N. V. Smith, Phys. Rev. B 2, 2840 (1970).
[13]Note that the scale in Fig. 5 for Cs is different from that presented earlier by Smith and Spicer in Ref. 6. The earlier EDCs were normalized to incorrect yield data. The scale of Fig. 5 above is to be regarded as the correct one.
[14]The photoemission properties of a nearly-free-electron metal had been worked out previously by H. Y. Fan [Phys. Rev. 68, 43 (1945)] and by H. Mayer and H. Thomas [Z. Physik 147, 419 (1957)].
[15]F. S. Ham, Phys. Rev. 128, 82 (1962).
[16]L. Sutton, Phys. Rev. Letters 24, 386 (1970).
[17]N. W. Ashcroft and W. L. Schaich, Proceedings of the Symposium on the Electronic Density of States, National Bureau of Standards, Gaithersburg, Maryland, 3–6 November 1969 (unpublished).
[18]G. D. Mahan, Phys. Rev. B 2, 4334 (1970).
[19]U. S. Whang, E. T. Arakawa, and T. A. Callcott, Phys. Rev. Letters 25, 646 (1970).
[20]K. Mitchell, Proc. Roy. Soc. (London) 146A, 442 (1934).
[21]J. C. Sutherland, R. N. Hamm, and E. T. Arakawa, J. Opt. Soc. Am. 59, 1581 (1969).
[22]J. J. Quinn, Phys. Rev. 126, 1453 (1962).
[23]H. Thomas, Z. Physik 147, 395 (1957).
[24]Note that the expressions and numerical values for l_i given in the previous paper (Ref. 1) are in error. The correct expressions are given by Eqs. (10) and (11) above.
[25]R. K. Nesbet and P. M. Grant, Phys. Rev. Letters 19, 222 (1967).
[26]L. Hedin, B. I. Lundqvist, and S. Lundqvist, in Ref. 17.
[27]A. U. MacRae, K. Müller, J. J. Lander, J. Morrison, and J. C. Phillips, Phys. Rev. Letters 22, 1048 (1969).
[28]We use the photoemission results for Cs rather than those for Na (Ref. 1). Due to the limited energy range, the surface-plasmon structure was not observable in the photoemission EDCs on Na.
[29]F. J. Piepenbring, in *Proceedings of the International Colloquium on the Optical Properties and Electronic Structure of Metals and Alloys*, edited by F. Abeles (North-Holland, Amsterdam, 1966), p. 316.

PHYSICAL REVIEW B VOLUME 3, NUMBER 11 1 JUNE 1971

Molecular-Orbital Model for KCl : Tl

D. Bramanti and M. Mancini
Istituto di Fisica Superiore dell'Università di Firenze, Firenze, Italy

and

A. Ranfagni
Istituto di Ricerca sulle Onde Elettromagnetiche del Consiglio Nazionale delle Ricerche, Firenze, Italy

(Received 31 March 1970; revised manuscript received 4 January 1971)

A semiempirical molecular-orbital calculation is developed for describing the energy levels of KCl : Tl. This approach is conceptually more satisfactory than the ionic one, as the nature of a Tl-Cl bond is largely covalent. The computations are first carried out in the one-electron approximation, and then the Coulomb and spin-orbit interactions are taken into account. No attempt is made at an exact calculation, but it is demonstrated that the covalent calculation gives a consistent interpretation of the absorption spectrum.

I. INTRODUCTION

The absorption spectrum characteristic of Tl^+ in alkali halide crystals consists of four bands labeled *A*, *B*, *C*, and *D*. The *A*, *C*, and *D* bands are strong and rather temperature independent, whereas the strength of the weaker *B* band is temperature dependent. The *A*, *B*, and *C* bands arise from transitions to excited states of the activator, whereas the *D* band is due to excited states of the host crystal (perturbed excitons).[1,2] The *A*, *B*, and *C* bands are qualitatively explained by the model proposed by Seitz,[3] and quantitative approaches to the problem of determining them were taken by Williams[4] on the basis of the ionic model. However, it was suggested[5,6] that a purely ionic description of the luminescence center was erroneous, and that modifications would have to be made to ob-